NATIONAL AERONAUTICS AND SPACE ADMINISTRATION
U.S.A.

HIGH-TEMPERATURE X-RAY-DIFFRACTOMETER STUDY OF OXIDATION OF TWO SUPERALLOYS, WI-52 AND IN-100

by Carl E. Lowell and Isadore L. Drell

Lewis Research Center
Cleveland, Ohio

1. Report No. NASA TM X-2002	2. Government Accession No.	3. Recipient's Catalog No.
4. Title and Subtitle HIGH-TEMPERATURE X-RAY-DIFFRACTOMETER STUDY OF OXIDATION OF TWO SUPERALLOYS, WI-52 AND IN-100		5. Report Date April 1970
		6. Performing Organization Code
7. Author(s) Carl E. Lowell and Isadore L. Drell		8. Performing Organization Report No. E-5230
9. Performing Organization Name and Address Lewis Research Center National Aeronautics and Space Administration Cleveland, Ohio 44135		10. Work Unit No. 129-03
		11. Contract or Grant No.
12. Sponsoring Agency Name and Address National Aeronautics and Space Administration Washington, D.C. 20546		13. Type of Report and Period Covered Technical Memorandum
		14. Sponsoring Agency Code

15. Supplementary Notes

16. Abstract

Oxidation of the cobalt alloy WI-52 and the nickel alloy IN-100 in air for 100 hr was studied by high-temperature X-ray diffraction. Polished WI-52 at 1600° to 2000° F (1144 to 1366 K) initially formed oxide scales of predominantly CoO, followed by $CoCr_2O_4$ formation. Ground and lapped WI-52 initially formed Cr_2O_3, followed by rapid CoO and $CoCr_2O_4$ formation. At 1900° F (1311 K) the scale of IN-100 after 100 hr had $NiTiO_3$ and $NiAl_2O_4$ as major phases; at 1700° and 1500° F (1200 and 1089 K) NiO was the major phase.

17. Key Words (Suggested by Author(s)) High-temperature Alloy X-ray Superalloy Diffractometer Oxides Oxidation Nickel Cobalt		18. Distribution Statement Unclassified - unlimited		
19. Security Classif. (of this report) Unclassified	20. Security Classif. (of this page) Unclassified		21. No. of Pages 20	22. Price* $3.00

HIGH-TEMPERATURE X-RAY-DIFFRACTOMETER STUDY OF

OXIDATION OF TWO SUPERALLOYS, WI-52 AND IN-100

by Carl E. Lowell and Isadore L. Drell

Lewis Research Center

SUMMARY

High-temperature X-ray diffraction was used to investigate the oxidation of two superalloys, the cobalt alloy WI-52 and the nickel alloy IN-100, in static air for 100 hours. The WI-52 exhibited the formation of four oxides: CoO, $CoCr_2O_4$, Cr_2O_3, and $Co_4Nb_2O_9$. When this alloy was oxidized in air at temperatures from 1600° to 2000° F (1144 to 1366 K) after metallographic polishing, CoO was initially the predominant oxide with $CoCr_2O_4$, Cr_2O_3, and $Co_4Nb_2O_9$ as minor phases. With time, the $CoCr_2O_4$ diffraction pattern increased while that of CoO decreased. At 2000° F (1366 K) and after about 10 hours the CoO intensity again began to increase. Ground and lapped surfaces promote an initial Cr_2O_3 layer followed by $CoCr_2O_4$ and then by an increasing predominance of CoO. Upon cooling, the CoO transforms to Co_3O_4.

Seven oxides were found on IN-100 oxidized in air at temperatures from 1500° to 1900° F (1089 to 1311 K). They were NiO, $NiCr_2O_4$, $NiTiO_3$, $NiAl_2O_4$, α-Al_2O_3, Cr_2O_3, and TiO_2. The oxides Cr_2O_3 and α-Al_2O_3 were found only in minor amounts. The TiO_2 was a major phase only at 1700° F (1200 K) for less than 10 hours. The NiO predominated at 1500° and 1700° F (1089 and 1200 K) after 3 and 10 hours, respectively, while $NiTiO_3$ and $NiAl_2O_4$ were the major phases at 1900° F (1311 K) after 50 hours.

INTRODUCTION

Material requirements for jet engines are becoming increasingly severe. Specifically, use temperatures are increasing. Designers would like to increase them even more. While the demand for higher use temperatures is usually interpreted in terms of strength, inadequate oxidation resistance is becoming the limiting factor. The materials consistently chosen for use at these higher temperatures are nickel- and cobalt-base superalloys. Usually the oxidation behavior of these materials is improved

through the use of coatings, but it is generally recognized that the use of coatings is a necessary evil. More desirable would be the improvement of the oxidation resistance of the superalloys themselves. To accomplish this goal, an understanding of the oxidation of these materials is highly desirable.

Unfortunately, the oxidation behavior of such superalloys is extremely complex. It cannot be understood by simply using the usual weight-gain techniques which have been at times successfully used on more simple systems. Such techniques do give some information as to how much and how fast oxidation takes place, but they give only indirect evidence as to what oxides are forming and in what sequence. This is especially important in superalloys where the formation of scales with more than five oxides is quite common.

One of the few methods available for identifying specific oxides in a scale is X-ray diffraction. It would seem then that a natural tool in oxidation analysis would be high-temperature X-ray diffraction (HTXRD). With this X-ray diffraction technique the course of the reactions can be followed at temperature, the sequence of formation of various oxides can be determined, and relative amounts of the oxides can be roughly estimated. While HTXRD has been used in oxidation in the past (e.g., refs. 1 to 3), the use has not been extensive. This report describes the application of HTXRD to the oxidation of two superalloys in an effort to contribute to the understanding of the process. The alloys were WI-52 (cobalt-base alloy) and IN-100 (nickel-base alloy). These alloys were chosen as being typical of cast alloys in current use in jet engines.

The oxides formed on the alloys under investigation were followed as a function of time (up to 100 hr) and temperature (up to 2000° F (1366 K) for WI-52 and 1900° F (1311 K) for IN-100). Both identification of the oxides and the relative intensity of their diffraction patterns were followed. This information is not only useful in itself, but can also be combined with other techniques to lead to a better understanding of those complex oxidation processes.


MATERIALS AND PREPARATION

Both alloys were received as cast coupons 1 by 2 by 0.1 inch (2.5 by 5.1 by 0.25 cm). Typical analyses from the heats used in this work are as follows:

Alloy	C	Mn	Si	P	S	Cr	Ni	W	Fe
IN-100	0.17	<0.1	<0.1	-----	0.003	9.70	Balance	----	0.11
WI-52	.47	.27	.27	0.015	.017	21.15	0.39	11.2	2.10

Alloy	Co	Mo	Al	Ti	Nb + Ta	Zr	B	V
IN-100	15.15	3.20	5.59	4.34	----	0.06	0.011	0.92
WI-52	Balance	----	----	----	1.73	----	-----	----

The microstructures of the as-cast material are shown in figures 1(a) and (b). The WI-52 consists of a solid solution of chromium (Cr), tungsten (W), iron (Fe), etc. in cobalt (Co), with (niobium, tungsten) carbide [(Nb, W)C], and metal carbides $M_{23}C_6$ and M_6C (M = Cr plus other metals such as W, Fe, Co, etc.) at the grain boundaries. The IN-100 is more complex. The major constituent is a precipitate of gamma prime $[\gamma' = Ni_3(Al, Ti)]$ in gamma (γ = Ni solid solution) which is typical of nickel-base super-alloys. At the grain boundaries are massive particles of γ' and titanium (carbon, nitrogen) [Ti(C, N)] (ref. 4). The depleted zone at the surface (fig. 1(b)) was removed in polishing before HTXRD.

Pieces 0.500 by 0.375 by 0.1 inch (1.27 by 0.95 by 0.25 cm) were cut from the coupons, keeping at least 0.1 inch (0.25 cm) from the edges. All samples of each alloy were cut from one coupon to avoid coupon-to-coupon variations in composition. All of the IN-100 samples and all but two of the WI-52 samples were polished successively with finer abrasive through 0.5-micron diamond and cleaned with acetone followed by methyl alcohol. The remaining two WI-52 samples were surface-ground and then hand-lapped with 6-micron diamond. Finally, flattened beads of platinum - platinum-13-percent-rhodium (Pt - Pt-13-percent-Rh) thermocouples made of 10-mil (0.025-cm) wire were spotwelded near the 0.375-inch (0.95-cm) edge on the prepared faces.
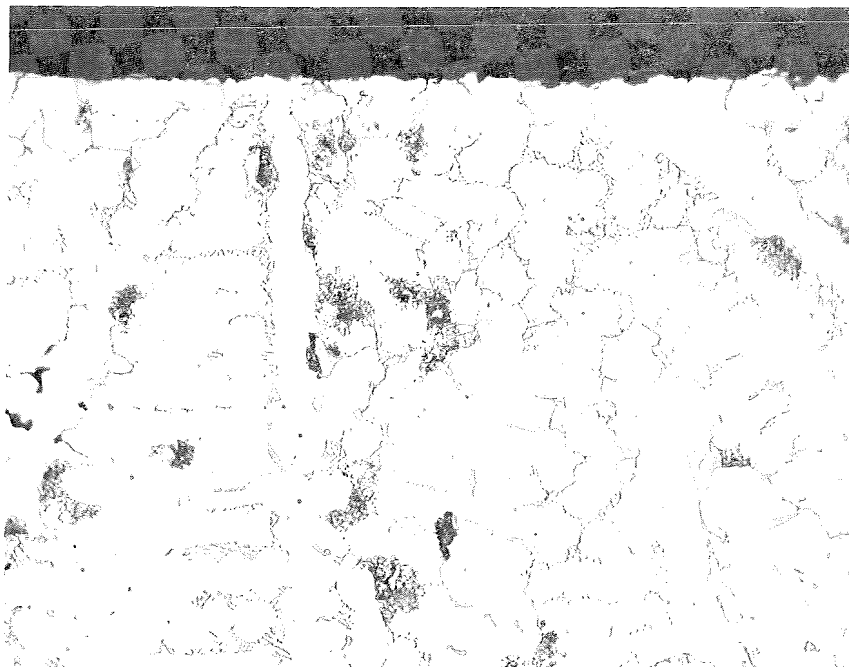
(a) Alloy, WI-52. Unetched.
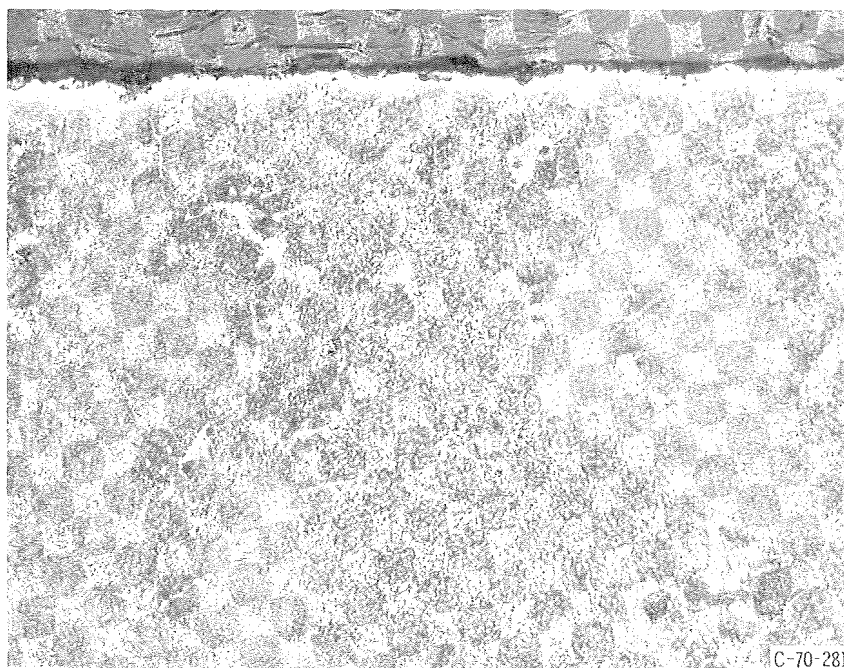
(b) Alloy, IN-100. Etchant: 33 percent H_2O; 33 percent acetic acid; 33 percent HNO_3; 1 percent HF.

Figure 1. - As-cast microstructures of WI-52 and IN-100. X250.

4

EQUIPMENT

Figure 2 is an overall view of the HTXRD apparatus used. It consists of a vertical goniometer, a lithium fluoride (LiF) monochromator in the diffracted beam, and a scintillation counter. Mounted on the diffractometer axis is a water-cooled aluminum chamber with 1/4-mil (0.0006-cm) mylar windows. As indicated in figure 3, the sample fits into a recess formed in a platinum strip heater which is in turn clamped to water-cooled electrodes. The electrodes are supported by an insulating platform whose height may be adjusted to keep the upper surface of the sample in proper alinement. The height adjustment and rotational alinement is made initially with the aid of a mica flake placed atop the sample. The adjustments are changed until the (004) reflection of the mica has a maximum intensity and is at the correct angle. After correct alinement is achieved, the mica flake is removed and the surface is viewed on edge with the binocular microscope shown in figure 2 and the cross hairs positioned so that their intersection is at the top surface of the sample. From this point until the end of the run the top surface is kept at the cross hair assuring accurate height adjustment even though the sample thickness changes as oxidation occurs. Temperature variations of the thermocouple on the sample were recorded during each run and were less than $\pm5^{\circ}$ F (3 K).

The X-ray source is a high-intensity copper-target tube capable of continuous operation at 40 kilovolts and 40 milliamps. The generator is rated at 2.5 kilowatts and has
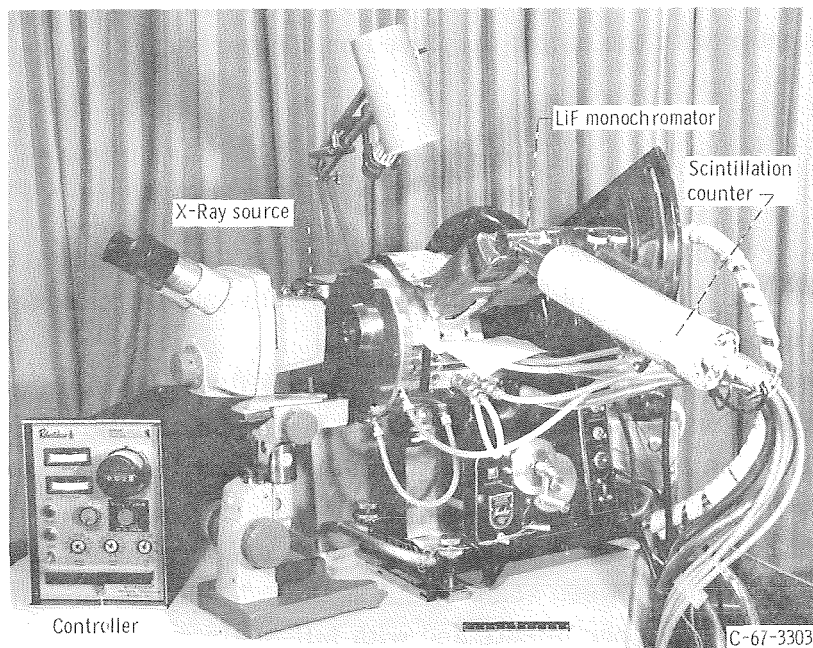

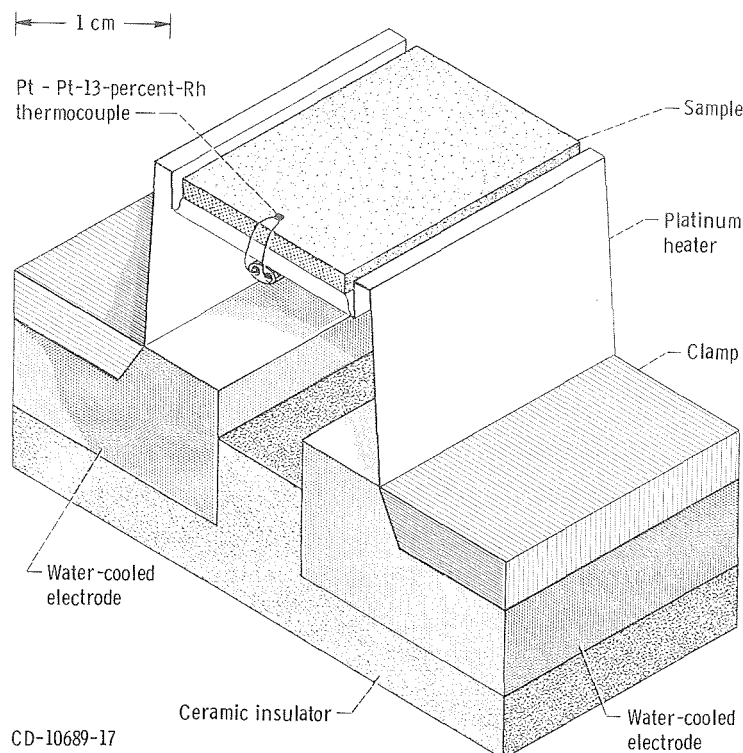Figure 2. - Overall view of high-temperature X-ray diffraction apparatus.

Figure 3. - Detail of heater-sample arrangement.

a constant-potential output. The signal from the scintillation counter is fed into a standard electronic detector with the output displayed on a recorder.

PROCEDURE

After surface preparation and the spot welding of the thermocouple, the sample was mounted on the heater. The height and rotational adjustments were made and a room-temperature diffractogram was run.

The oxidation runs were initiated by heating rapidly (less than 5 min) to temperature. Immediately, a diffractometer scan was started at 2^O 2θ per minute. The first few scans covered only a limited range in the front-reflection region, for example 20° to 60° 2θ, and they were run one immediately after the other. As the rate of change of oxide intensity slowed down, longer scans were made covering angles as low as 12° and up to 152° 2θ, and the time between scans was lengthened. Slower scanning speeds were used overnight, $1/8^O$ 2θ per minute and with full-scale ranges as low as 25 counts per second, to bring out the weaker peaks above the background (which was of the order of a few counts per second, with major oxide peaks up to a few hundred counts per

6

second). Oxidation proceeded uninterrupted for about 100 hours after which the temperature was reduced in steps to 1500° F (1089 K), 1000° F (811 K), 500° F (533 K), and finally room temperature. At each of these temperatures, a pattern was made to look for possible phase changes.

After removal from the chamber, the samples were mounted partially in epoxy. The part of the sample sticking out of the epoxy was scraped to obtain powder samples which were run in a Debye camera to check for the presence of minor oxide phases that might have escaped detection in the diffractometer. The protruding part of the sample was then cut off leaving a sectioned piece in the epoxy. The section was then polished and examined metallographically.

After the identification of the phases present, the peak heights (above background) of the major peaks were plotted against time. The use of peak heights rather than integrated intensities to estimate the relative abundance of the phases present was deemed adequate for the purposes of this investigation in view of the many approximations involved, some of which are discussed subsequently. These plots are used to show rough trends only; they are not meant to give a quantitative measure of the amounts present.

RESULTS AND DISCUSSION

General

Plots of peak height against time for runs made at 1500° to 2000° F (1089 to 1366 K) are shown in figures 4 to 6. Interpretation of these results must be accompanied by an understanding of the following factors which, if ignored, tend to mislead one. Because the scale is examined in situ and the oxide tends toward a layered structure, oxides which are near the gas-oxide interface have more intense diffraction patterns than those near the oxide-metal interface. Also, preferred orientation in the oxide can either enhance or diminish the intensity of a single line. This can be even a greater problem if the orientation changes during the course of a run. In the present work, preferred orientation was not present in the oxides to any great degree. This was determined by comparing the relative intensities obtained for each oxide with its corresponding card in the ASTM powder diffraction file. However, the large grain size of CoO formed at high temperature and/or long oxidation times did cause misleading intensities which are discussed later. Preferred orientation was, however, a distinct factor in the intensities of the metal solid solutions. Fortunately, these intensities were needed only to determine whether or not increasing adsorption of the X-ray beam by the oxide layer prevented the beam from penetrating through the entire layer. In addition, little if any change in the orientation occurred during the runs. Layering was
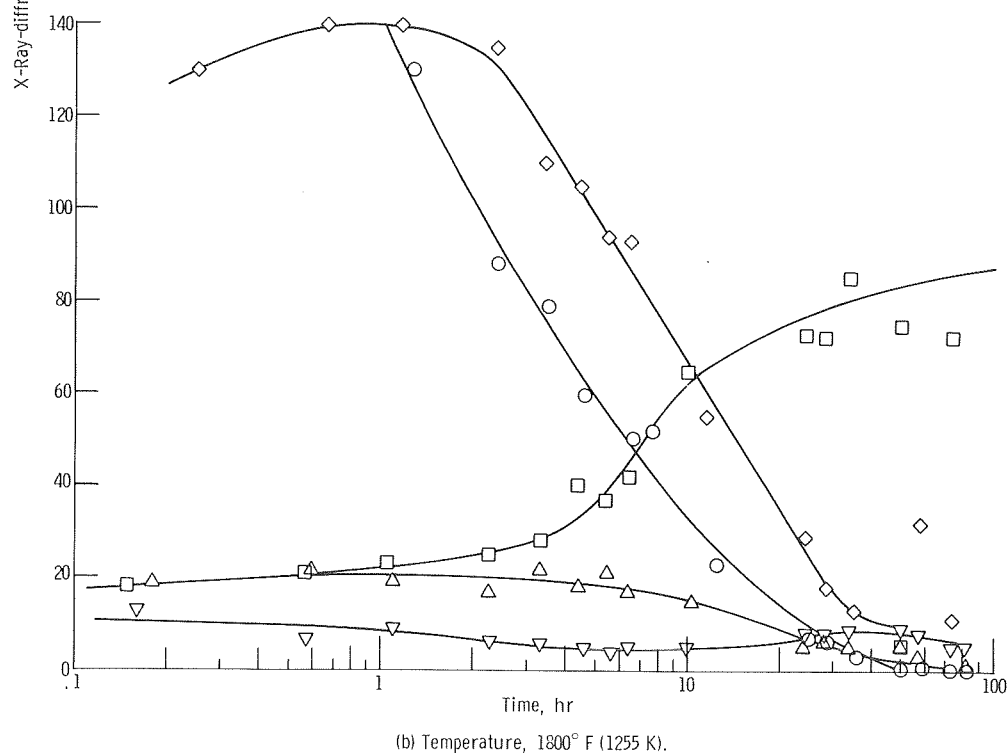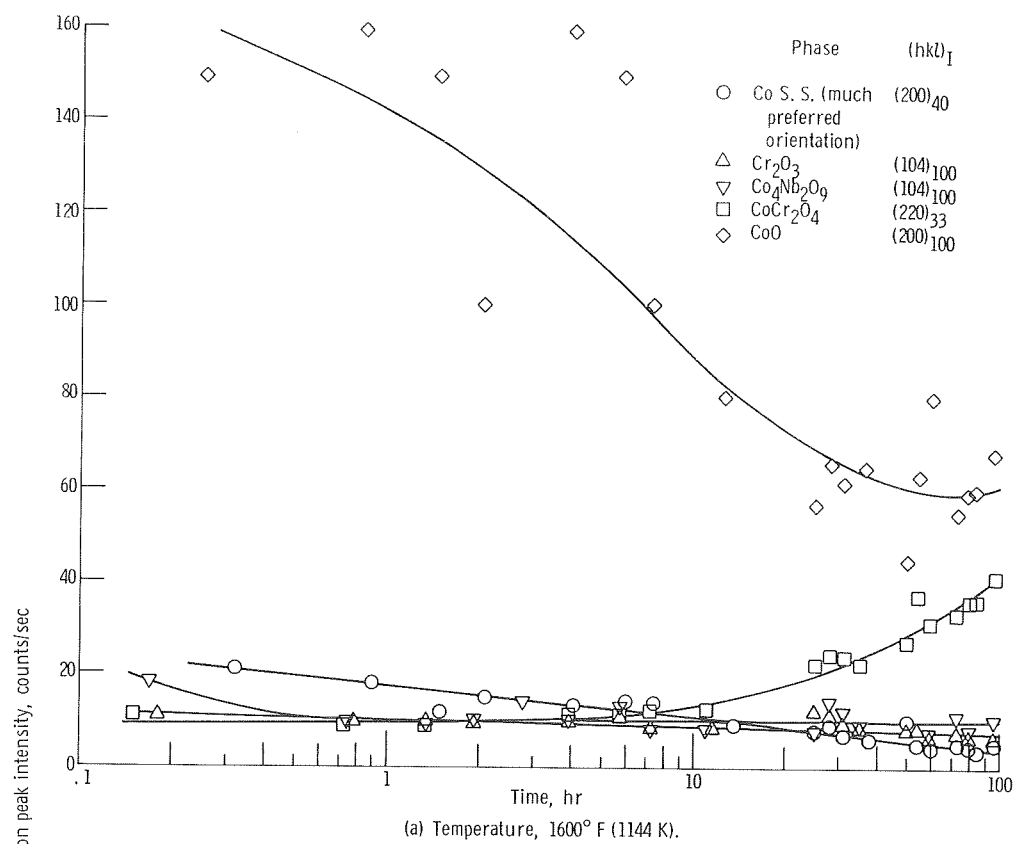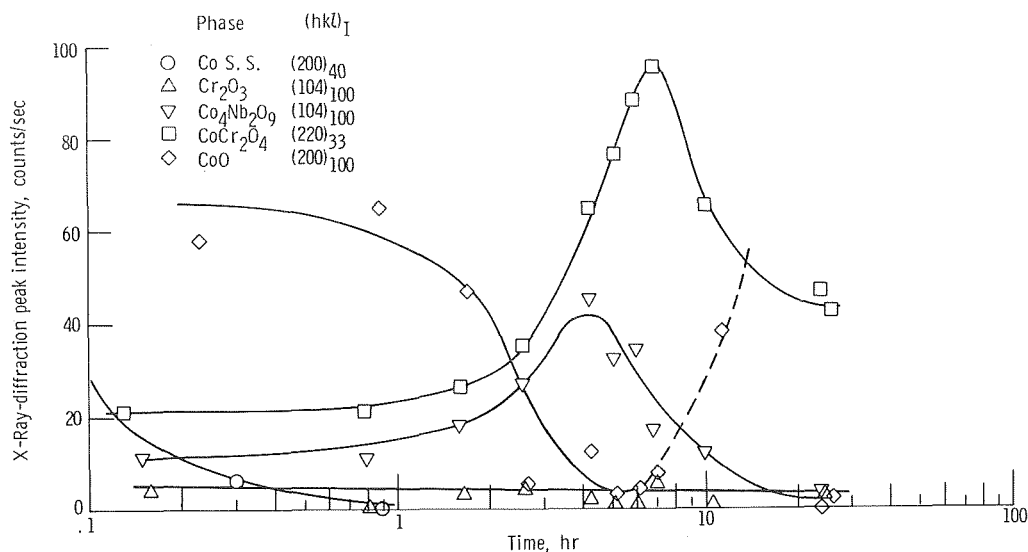
7

Phase		$(hkl)_I$
○	Co S. S. (much preferred orientation)	$(200)_{40}$
△	Cr_2O_3	$(104)_{100}$
▽	$Co_4Nb_2O_9$	$(104)_{100}$
□	$CoCr_2O_4$	$(220)_{33}$
◇	CoO	$(200)_{100}$

(a) Temperature, 1600° F (1144 K).

(b) Temperature, 1800° F (1255 K).

Figure 4. - Oxidation of polished WI-52 in air.

8

Figure 4. - Concluded.

a significant problem whose effects could be only qualitatively assesed by post-oxidation metallography.

The diffraction peaks chosen in plotting the results (see figs. 4 to 6) were not always the strongest for each phase but rather the strongest peaks free of any extensive interference from peaks of other phases. The relative intensities listed in the ASTM powder diffraction file for the line used are shown on the graphs as an aid in estimating the relative strengths of the oxide diffraction patterns. It should be kept in mind that the oxide formulae used in this report are simplifications; in reality, many minor cations are in solution in these oxides and could affect intensities.

In the case of the IN-100 plots, the intensities of the oxide peaks were multiplied by the factors shown in figure 6. This is equivalent to comparing all oxide patterns on the basis of their strongest lines (i. e. , the line with an intensity of 100) in the ASTM file. One more change in the intensities was made. The NiO peak intensities were divided by two in the 1900° plot (fig. 6(c)) to keep them on scale without compressing the other curves drastically.
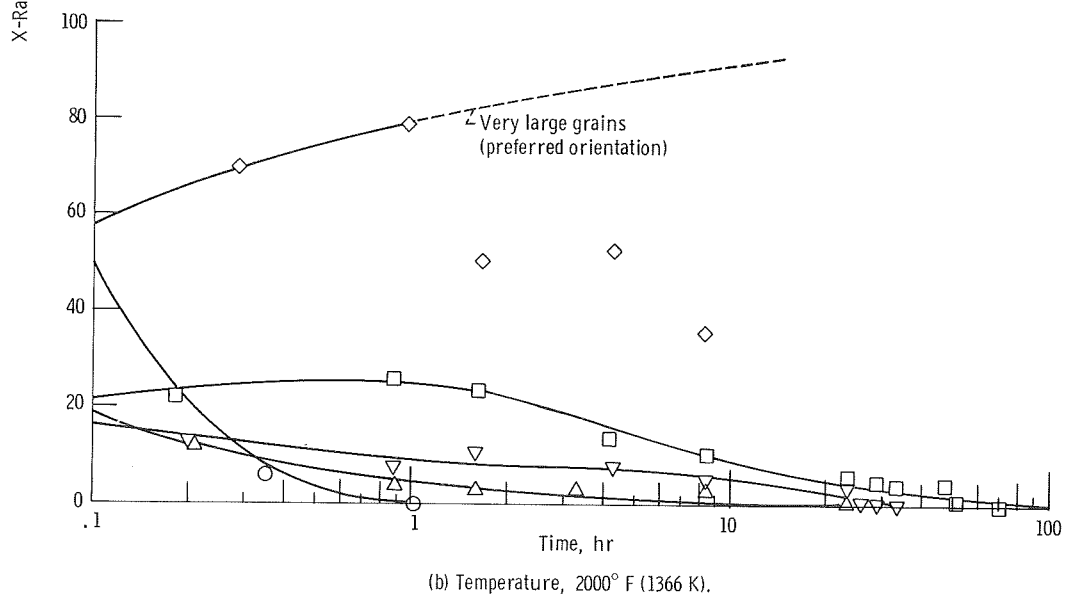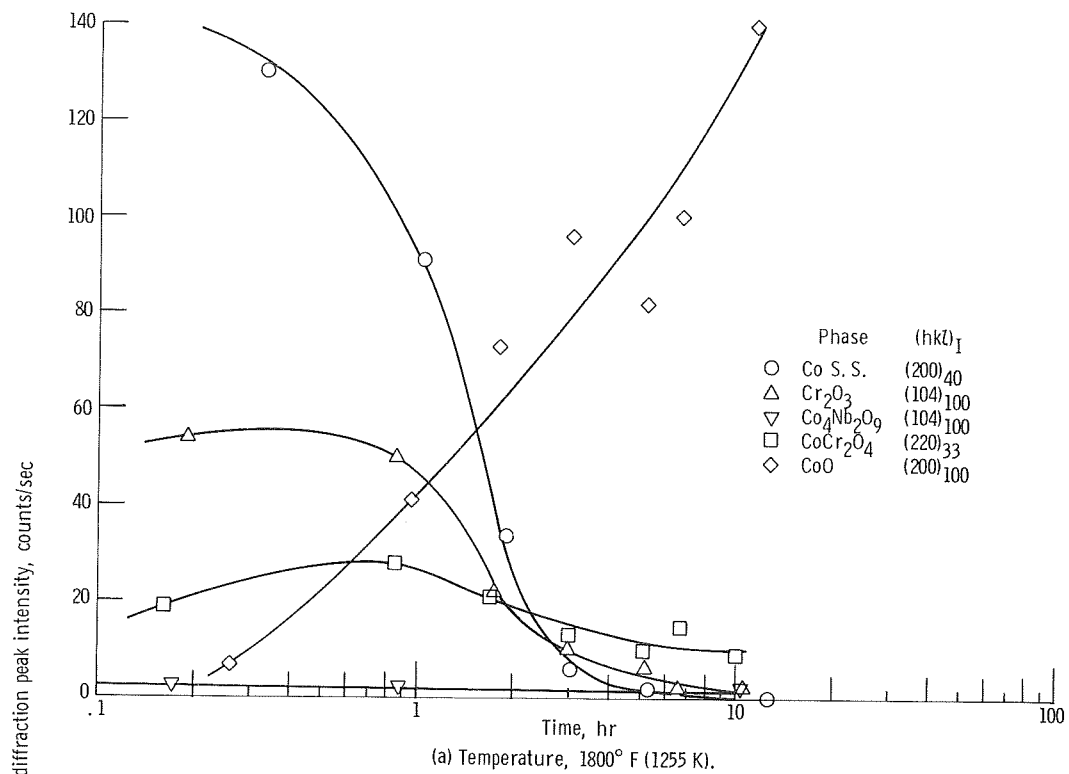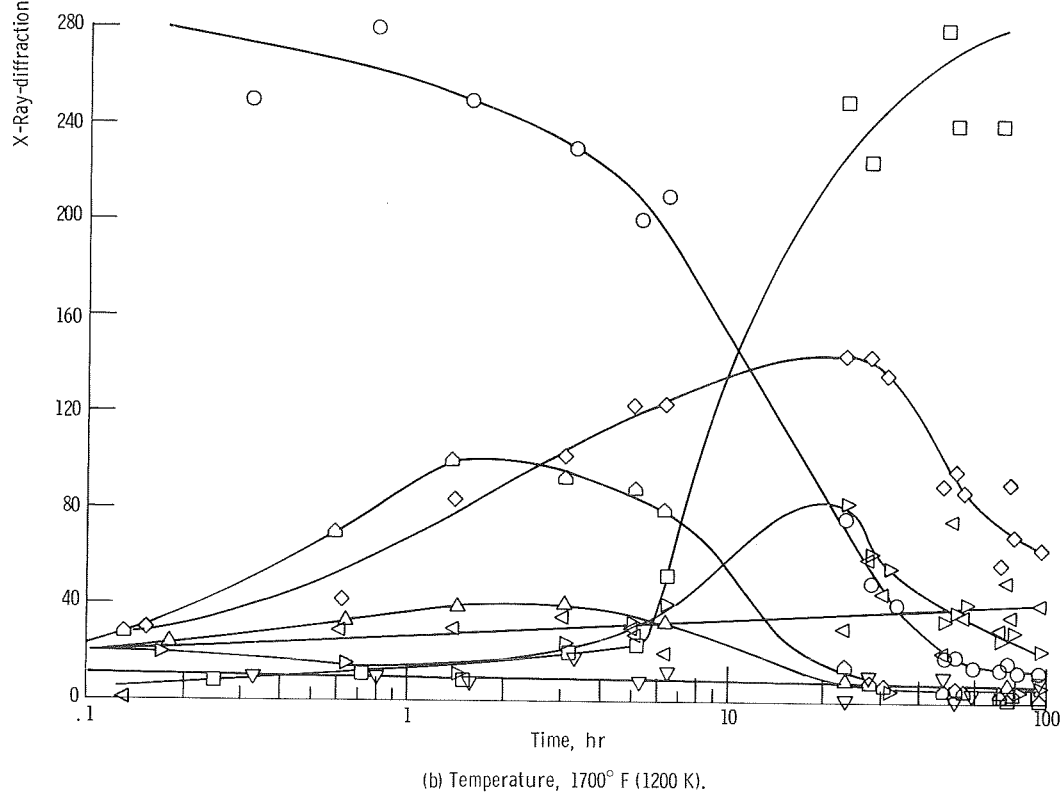
Figure 5. – Oxidation of ground and lapped WI-52 in air.
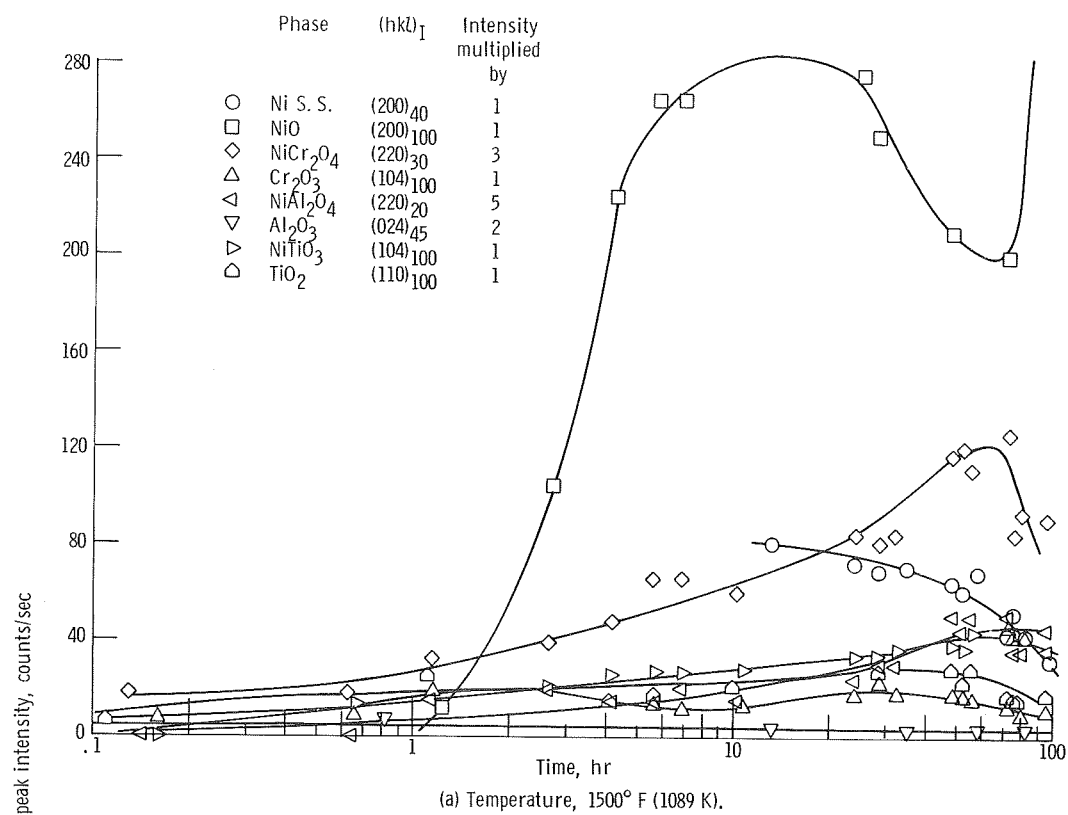
Figure 6. - Oxidation of IN-100 in air.

(a) Temperature, 1500° F (1089 K).

(b) Temperature, 1700° F (1200 K).

Phase	(hkl)$_I$	Intensity multiplied by
○ Ni S.S.	(200)$_{40}$	1
□ NiO	(200)$_{100}$	1
◇ NiCr$_2$O$_4$	(220)$_{30}$	3
△ Cr$_2$O$_3$	(104)$_{100}$	1
◁ NiAl$_2$O$_4$	(220)$_{20}$	5
▽ Al$_2$O$_3$	(024)$_{45}$	2
▷ NiTiO$_3$	(104)$_{100}$	1
△ TiO$_2$	(110)$_{100}$	1

Phase	$(hkl)_I$	Intensity multiplied by
○ Ni S. S.	$(200)_{40}$	1
□ NiO	$(200)_{100}$	1/2 - (Reduction in intensity to keep on scale)
◇ $NiCr_2O_4$	$(220)_{30}$	3
△ Cr_2O_3	$(104)_{100}$	1
◁ $NiAl_2O_4$	$(220)_{20}$	5
▽ Al_2O_3	$(024)_{45}$	2
▷ $NiTiO_3$	$(104)_{100}$	1
△ TiO_2	$(110)_{100}$	1

(c) Temperature, 1900° F (1311 K).

Figure 6. - Concluded.

Oxidation of WI-52

All HTXRD runs on WI-52 showed the same collection of phases: CoO, $CoCr_2O_4$, Cr_2O_3, $Co_4Nb_2O_9$, and cobalt solid solutions. It is noted that no tungsten oxides were found. The CoO, $CoCr_2O_4$, and Cr_2O_3 arise mainly from the oxidized matrix, while the $Co_4Nb_2O_9$ is probably due to the reaction of matrix Co with the grain boundary (W, Nb)C and oxygen. The oxide is probably $Co_4(Nb, W)_2O_9$ since tungsten oxides are soluble in niobium oxides (ref. 5) and no tungsten oxides were found.

12

At 1600° F (1144 K), CoO is the only oxide formed in large quantity on polished WI-52 (see fig. 4(a)) under the test conditions used in this study. However, small amounts of Cr_2O_3, $Co_4Nb_2O_9$, and $CoCr_2O_4$ are present. With time the CoO decreases. The peak intensity decreases until at 100 hours its value is less than one-half that at 1 hour. During the same interval, the $CoCr_2O_4$ peak intensity increases nearly fourfold.

Figure 4(b) shows the data obtained from oxidation at 1800° F (1255 K). The trends in the oxide curves are similar to those at 1600° F (1144 K). However, the rates of change are much faster (nearly a factor of 10). After 50 hours at temperature, the intensity of the CoO pattern becomes erratic. This may be due to a tendency for the formation of a few large CoO crystals on the surface.

At 2000° F (1366 K) the same trends (fig. 4(c)) are seen as at the lower temperatures. As before, an increase of 200° F (111 K) decreases the time required to reach a similar oxidation stage by almost a factor of 10. At this temperature the $CoCr_2O_4$ goes through a maximum. At the same time as the $CoCr_2O_4$ maximum the CoO intensities again become erratic. At this point, large crystal facets were observed through the microscope. This combined with the metallography evidence to be discussed later indicates that the actual amount of CoO begins to increase at this point even if the X-ray intensity values are ambiguous. The overlaying by the CoO and its resultant absorption is the cause for the decrease in the $CoCr_2O_4$ signal. Note that the $Co_4Nb_2O_9$ also increases and goes through a maximum at a time similar to the $CoCr_2O_4$, indicating that the CoO is growing over the grain boundaries as well as the matrix. The run ended after 25 hours when the heater failed as a result of a hot spot, a frequent occurrence at this temperature.

At 2000° F (1366 K) the diffraction pattern of the cobalt solid solution disappeared after 1 hour. This was peculiar to this temperature. At lower temperatures the solid solution pattern was still present at the end of the run. At 1600° F (1144 K) the low apparent intensities of the cobalt solid-solution pattern in figure 4(a) were due to the preferred orientation referred to previously.

All samples showed an oxide phase change upon cooling to 1500° F (1089 K). The CoO transforms (ref. 6) into a self-spinel internally to a small degree:

$$CoO_{1+x} \rightarrow (1-3x)\ CoO + x\ Co_3O_4 \qquad (1)$$
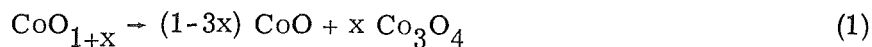
In contrast, the oxides on the surface react with oxygen:

$$3CoO + \frac{1}{2} O_2 \rightarrow Co_3O_4 \qquad (2)$$

13

Some spallation occurred upon cooling to room temperature. Room-temperature Debye camera patterns of powders scraped from the 2000° F (1366 K) run showed small amounts of another oxide phase in the scale - $CoWO_4$.

Metallographic examination of the samples confirmed the position of the oxides deduced from HTXRD. Figure 7 shows the layered arrangement of the oxides. At the metal-oxide interface is a thin layer of Cr_2O_3 with its characteristic green color revealed by polarized light. The next oxide layer is mostly $CoCr_2O_4$, probably with some $CoWO_4$. This is inferred by the observation of a blue-green phase in the spinel under
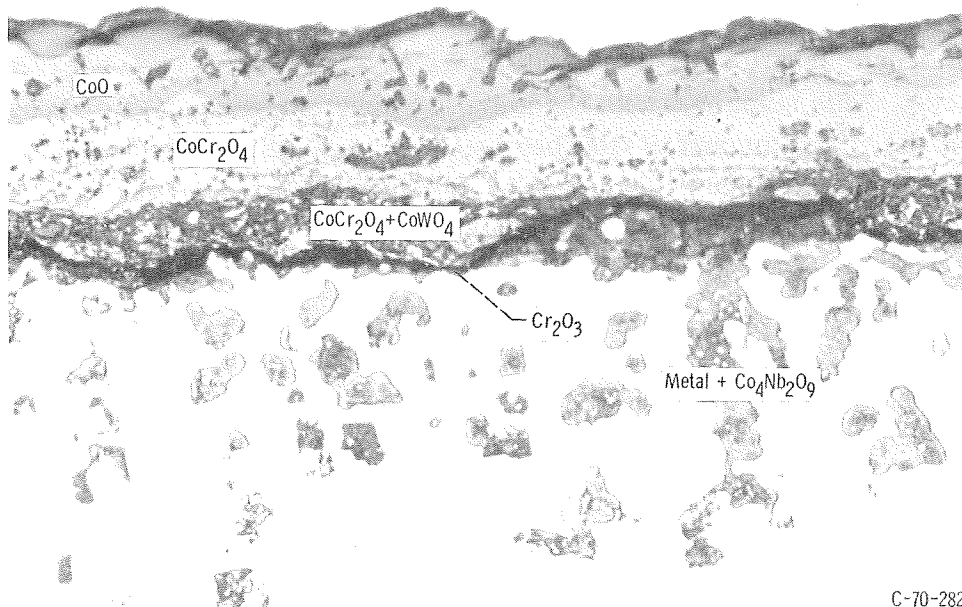

Figure 7. - Microstructure of oxidized polished WI-52. Time, 100 hours; temperature, 2000° F (1366 K). X500.

polarized light and the fact that $CoWO_4$ was found in small amounts by room-temperature XRD. The layer at the oxide-gas interface contains large-grained CoO and small amounts of Co_3O_4. Figure 8 shows a similar layer of another sample in detail. It can be seen that the Co_3O_4 is formed by precipitation within grains, by oxidation of exposed CoO surfaces, and perhaps by grain-boundary oxidation. However, the latter may really be oxidation at cracks in the CoO. This demonstrates that both reactions postulated previously are valid.
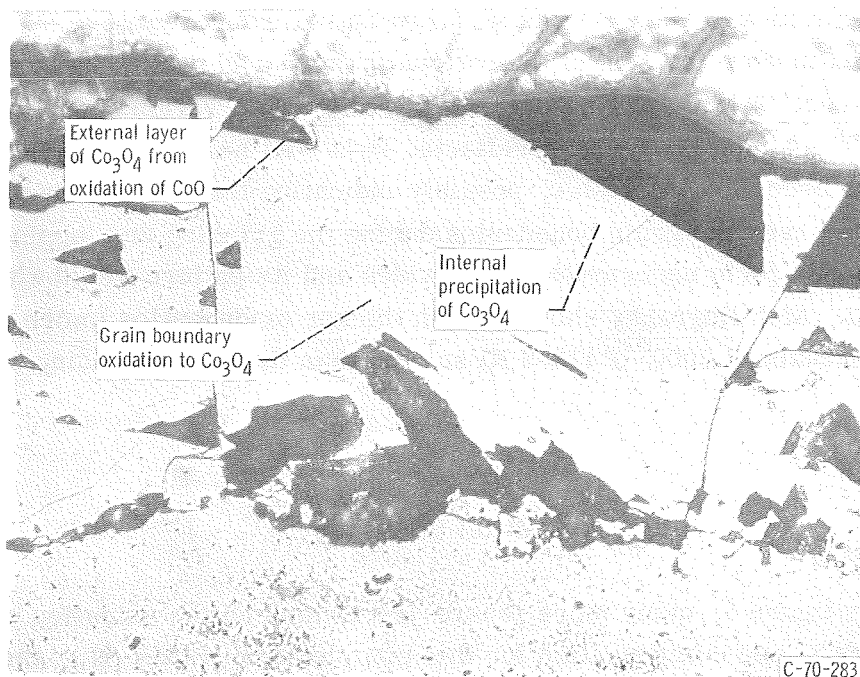
14

Figure 8. - Top oxide layer of polished WI-52. Time, 100 hours; temperature, 2000° F (1366 K). X350.

The oxidation of WI-52 polished surfaces as gleaned from HTXRD may be summarized as follows:

(1) Initially CoO is formed on the surface along with small amounts of Cr_2O_3 and $Co_4Nb_2O_9$ at the grain boundaries.

(2) The CoO reacts with Cr_2O_3 to form $CoCr_2O_4$. This is seen from the decrease in the CoO intensity which cannot be accounted for by overlaying inasmuch as it is at the surface.

(3) As the initially rapid $CoCr_2O_4$ formation rate diminishes, the CoO layer again grows, overlaying the rest of the oxides and causing their intensities to decrease even though they probably continue to grow.

(4) Upon cooling, part of the CoO transforms to Co_3O_4 with a 10-percent volume contraction (for a constant amount of oxygen). This transformation probably contributes to spallation of WI-52 upon cooling.

The oxidation of ground and lapped surfaces of WI-52 were also investigated by HTXRD. The same procedures were used as with the polished samples. All the samples were cut from the same casting coupon. At 1800° F (1255 K) (see fig. 5(a)) Cr_2O_3 is the strongest initial oxide followed by $CoCr_2O_4$ with very little, if any, CoO. After 1 hour, the CoO starts to form in large quantities and overlays the Cr_2O_3 and $CoCr_2O_4$ causing their intensities to fall off. At 2000° F (1366 K) (see fig. 5(b)) the process is so ac-

15

celerated that by 0.1 hour the CoO has completely dominated the diffraction patterns. In 1 hour the grain size of the CoO was so large that no representative pattern was obtained for it, and in time the rest of the pattern disappeared due to the overlaying of CoO. The presence of large grains was confirmed by observation of the surface through the binocular microscope viewed with reflected light. At neither temperature did the $Co_4Nb_2O_9$ phase become appreciable, possibly indicating that the relatively soft matrix had been smeared over the grain boundaries during the grinding and lapping. In this way the $Co_4Nb_2O_9$ would form underneath other oxides and its pattern would always be heavily overlaid. Metallography showed much thicker oxide scales (more than tenfold) on the ground and lapped 2000° F (1366 K) sample than the corresponding polished sample.

Oxidation of IN-100

As shown in figure 6, many more phases are formed on the oxidation of IN-100 than of WI-52. There is one compensation for this complexity. Nickel (Ni), the major element in the alloy and scale, absorbs CuK_{α} radiation much less than the Co of WI-52. Therefore, the effect of layering on the oxide is much reduced in IN-100. This is evident from the fact that some signal from the nickel solid solution is present after 100 hours at 1900° F (1311 K). In WI-52 the signal from the cobalt solid solution is gone in less than 50 hours at 1800° F (1255 K).

After a few hours at 1500° F (1089 K) (see fig. 6(a)) only one oxide is present in high concentration - NiO. Up to 1 hour after oxidation began, NiO was not detected, and the scale consists of TiO_2, $NiCr_2O_4$, $NiTiO_3$, $NiAl_2O_4$, and Cr_2O_3. After 1 hour these scale constituents increase slightly while the NiO is initiated and increases very rapidly to dominate the oxide patterns. At approximately 50 hours the NiO goes through a minimum and the $NiCr_2O_4$ a maximum in a fashion similar to the monoxide and spinel on WI-52, which may be ascribed to a similar cause.

Increasing the temperature to 1700° F (1200 K) (see fig. 6(b)) changes the oxidation pattern markedly. An initially intense TiO_2 pattern is obtained which more than doubles in intensity in 2 to 3 hours, but then falls off rapidly after 10 hours. While the TiO_2 pattern was diminishing, $NiTiO_3$ was going through a maximum, perhaps an indication of the reaction of TiO_2 with the NiO which has formed. The Cr_2O_3 follows a pattern similar to TiO_2, and $NiCr_2O_4$ follows one similar to $NiTiO_3$. Perhaps these are analogous situations. Both $NiAl_2O_4$ and Al_2O_3 start as, and remain, minor phases. The NiO, which at this temperature is present from the start, becomes the predominant oxide between 5 and 10 hours and from then on just continued to increase.

16

Increasing the temperature to 1900° F (1311 K) (fig. 6(c)) leads to another shift in the process of oxidation. Both NiO and $NiCr_2O_4$ dominate the oxide patterns from the start and increase to maximums near 10 hours. From then on their intensities decrease rapidly, and after 100 hours their intensities drop to near zero. The only other oxides in the first few hours were $NiTiO_3$ and $NiAl_2O_4$ which remain at a constant intensity for the first 10 hours. From that point on, the $NiTiO_3$ intensity increased continuously to 100 hours and the $NiAl_2O_4$ increased markedly. After 50 hours, $NiTiO_3$ is apparently the major phase. Throughout the entire run Cr_2O_3 or Al_2O_3 were very weak. Between 6 and 10 hours TiO_2 was identified.

At all temperatures a few weak lines were present which represent an unidentified phase or phases. This phase was not seen at long times at 1900° F (1311 K). A tentative identification of zirconium dioxide (ZrO_2) and possibly γ-Al_2O_3 was made, but the fit of the pattern with the ASTM powder data is not good.

In all IN-100 runs, patterns taken upon cooling to 1500° F (1089 K), 1000° F (811 K), 500° F (533 K), and room temperature showed no phase changes. In addition, room-temperature Debye powder patterns made from the scraped oxides showed no phases not identified by HTXRD.

Figures 9(a) and (b) show the microstructure of oxidized IN-100. At the lower temperature (fig. 9(a)) the NiO can be seen to be the dominant oxide and to be positioned at the gas-oxide interface. The rest of the oxide is a distribution of small crystallites of the other six oxides. At the higher temperature, figure 9(b) does not show a major oxide. All seven oxides are distributed as fine equiaxed grains. Apparently, some of the oxide spalled during mounting.

Unlike WI-52, the oxidation behavior of IN-100 cannot be easily summarized. This results from the different modes of oxidation at each temperature studied. The oxidation mechanism is complex. It is, however, dominated by NiO at long times at 1500° and 1700° F (1089 and 1200 K). At the highest temperature studies (1900° F (1311 K)), $NiTiO_3$ and $NiAl_2O_4$ are the major oxides, and they resulted in large part from the reaction of NiO with TiO_2 and Al_2O_3. If a way could be found to suppress NiO and induce Al_2O_3 to become the dominant oxide, the oxidation characteristics of this alloy might be enhanced.

The reasons for the complexity of the oxidation of IN-100 are speculative. The presence of the γ - γ' eutectic makes continuous oxide layers difficult to form. In addition, IN-100 contains three strong oxide-forming elements (Cr, Al, and Ti). However, much more work would be needed to determine the roles of these factors, and this research is beyond the scope of this report.
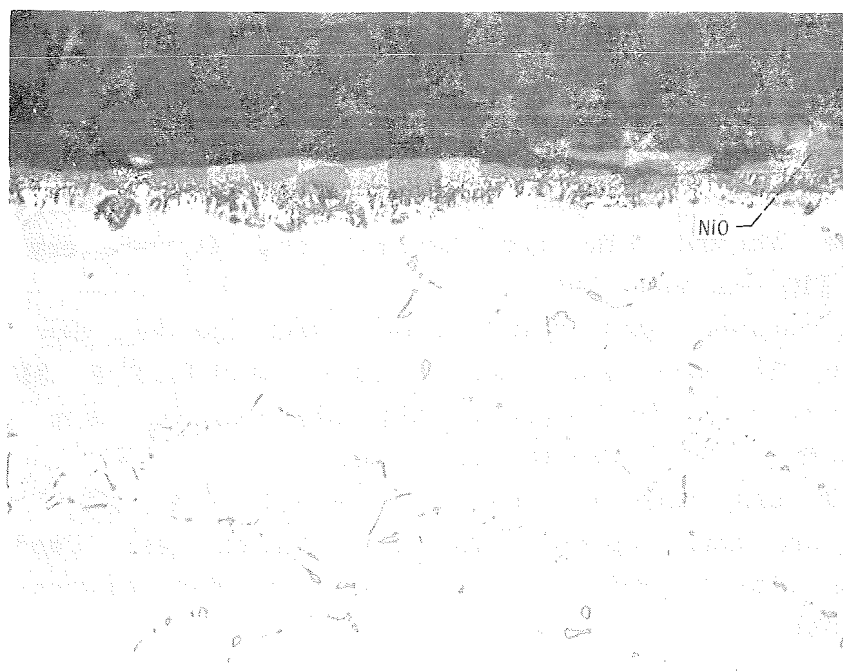
(a) Temperature, 1500° F (1089 K); unetched. X500.
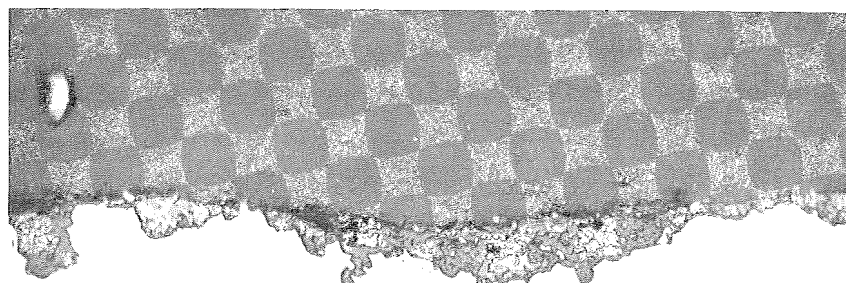
C-70-284

(b) Temperature, 1900° F (1311 K); unetched. X250.

Figure 9. – Microstructure of oxidized IN-100. Time, 96 hours.

CONCLUDING REMARKS

While HTXRD must be supplemented by other techniques before an understanding of the oxidation process can be achieved, much can be learned by its use. The oxidation of WI-52 showed no changes in reaction mechanism at temperatures of 1600° to 2000° F (1144 to 1366 K), only the usual increase of rates with temperature. However, surface preparation, which was studied only in this alloy, was found to be a major factor in the oxidation of WI-52. Polishing promotes spinel formation after an initial CoO dominance. Grinding followed by lapping promotes the formation of CoO after an initial Cr_2O_3 formation.

The oxidation of IN-100 is more complex than WI-52 either as a function of time or temperature. At 1500° and 1700° F (1089 and 1200 K), NiO is the dominant oxide by far in IN-100. The TiO_2 becomes a major phase only at 1700° F (1200 K). At 1900° F (1311 K), $NiTiO_3$ and $NiAl_2O_4$ become the major phases after 100 hours, whereas NiO was the major for the first 30 hours.

Lewis Research Center,
    National Aeronautics and Space Administration,
        Cleveland, Ohio, January 23, 1970,
           129-03.

REFERENCES

1. Goldschmidt, H. J.: An X-Ray High-Temperature Oxidation Study on Iron-Copper. J. Iron Steel Inst., vol. 196, pt. 4, Dec. 1960, pp. 390-393.

2. Kennedy, S. W.; Calvert, L. D.; and Cohen, M.: Oxidation of Three Iron-Nickel Alloys and Iron at 800° C. Trans. AIME, vol. 215, no. 1, Feb. 1959, pp. 64-72.

3. Norman, N.: Metallic Oxide Phases of Niobium and Tantalum. I. X-Ray Investigations. J. Less-Common Metals, vol. 4, no. 1, Feb. 1962, pp. 52-61.

4. Wlodek, S. T.: The Structure of IN-100. ASM Trans., vol. 57, no. 1, Mar. 1964, pp. 110-119.

5. Meerson, G. A.; and Panov, V. S.: Atmospheric Oxidation Resistance of WC-NbC-Co Alloys. Soviet Powder Met. Metal Ceramics, no. 8, Aug. 1967, pp. 645-648.

6. O'Bryan, H. M., Jr.; and Parravano, G.: The Univariant Equilibrium Between the Oxides of Cobalt. Reactivity of Solids. G. M. Schwab, ed., Elsevier Publ. Co., 1965, pp. 256-268.

"The aeronautical and space activities of the United States shall be conducted so as to contribute . . . to the expansion of human knowledge of phenomena in the atmosphere and space. The Administration shall provide for the widest practicable and appropriate dissemination of information concerning its activities and the results thereof."

— NATIONAL AERONAUTICS AND SPACE ACT OF 1958

NASA SCIENTIFIC AND TECHNICAL PUBLICATIONS

TECHNICAL REPORTS: Scientific and technical information considered important, complete, and a lasting contribution to existing knowledge.

TECHNICAL NOTES: Information less broad in scope but nevertheless of importance as a contribution to existing knowledge.

TECHNICAL MEMORANDUMS: Information receiving limited distribution because of preliminary data, security classification, or other reasons.

CONTRACTOR REPORTS: Scientific and technical information generated under a NASA contract or grant and considered an important contribution to existing knowledge.

TECHNICAL TRANSLATIONS: Information published in a foreign language considered to merit NASA distribution in English.

SPECIAL PUBLICATIONS: Information derived from or of value to NASA activities. Publications include conference proceedings, monographs, data compilations, handbooks, sourcebooks, and special bibliographies.

TECHNOLOGY UTILIZATION PUBLICATIONS: Information on technology used by NASA that may be of particular interest in commercial and other non-aerospace applications. Publications include Tech Briefs, Technology Utilization Reports and Notes, and Technology Surveys.

Details on the availability of these publications may be obtained from:

SCIENTIFIC AND TECHNICAL INFORMATION DIVISION

NATIONAL AERONAUTICS AND SPACE ADMINISTRATION
Washington, D.C. 20546